Noncontact Dipole Effects on Channel Permeation. III. Anomalous Proton Conductance Effects in Gramicidin

L. Revell Phillips,* Chad D. Cole,* Reed J. Hendershot,* Myriam Cotten,[#] Timothy A. Cross,[#] and David D. Busath*

*Zoology Department, Brigham Young University, Provo, Utah 84062, and [#]Center for Interdisciplinary Magnetic Resonance at the National High Magnetic Field Laboratory, Institute of Molecular Biophysics and Department of Chemistry, Florida State University, Tallahassee, Florida 32306 USA

ABSTRACT   Proton transport on water wires, of interest for many problems in membrane biology, is analyzed in side-chain analogs of gramicidin A channels. In symmetrical 0.1 N HCl solutions, fluorination of channel Trp^{11}, $Trp-^{13}$, or Trp^{15} side chains is found to inhibit proton transport, and replacement of one or more Trps with Phe enhances proton transport, the opposite of the effects on K^+ transport in lecithin bilayers. The current-voltage relations are superlinear, indicating that some membrane field-dependent process is rate limiting. The interfacial dipole effects are usually assumed to affect the rate of cation translocation across the channel. For proton conductance, however, water reorientation after proton translocation is anticipated to be rate limiting. We propose that the findings reported here are most readily interpreted as the result of dipole-dipole interactions between channel waters and polar side chains or lipid headgroups. In particular, if reorientation of the water column begins with the water nearest the channel exit, this hypothesis explains the negative impact of fluorination and the positive impact of headgroup dipole on proton conductance.

INTRODUCTION

Proton transport is a critical process in physical chemistry and biology, including ATP production (Girvin et al., 1998; Boyer, 1997), voltage-activated proton channels in epithelia (DeCoursey and Cherny, 1994), and light transduction (Lanyi, 1995). It is postulated to occur by a mechanism similar to one for salt-based conductivity suggested in 1805 by C. J. von Grotthuss (Moore, 1972) and is therefore termed Grotthuss conductance. Within aqueous channels proton transport occurs as covalent bonds exchange with hydrogen bonds between hydronium and a neighboring water to produce charge transport followed by a slower reorientation of the electroneutral water molecule. The gramicidin channel provides an ideal molecular system in which to explore the energetics and dynamics of the Grotthuss conductance. The results in this paper suggest that modulation of noncontact dipoles near the gramicidin permeation pathway allows one to dissect the oriented dipoles in a water column, distinguishing the motions of those near the back half of the channel from those in the front half.

Gramicidin A (gA) single-helix transmembrane channels are relatively featureless pores lined only by peptide backbone atoms, with symmetrical binding sites of moderate affinity near the entry and the exit. Alkali metal cation transport is considered in simplest terms to be carried out in three steps: two primarily extrachannel steps (diffusion through bulk aqueous solution up to the channel combined with entry into the binding site and exit from the exit site followed by aqueous diffusion away from the channel) and one intrachannel step (usually referred to as cation translocation). The rate of the intrachannel step is highly dependent on membrane potential, causing current-voltage relationships (*I-V*s) to be superlinear when the intrachannel step is rate limiting (Andersen, 1983; Hladky and Haydon, 1984; Busath et al., 1998). Thus *I-V*s are sublinear at low permeant ion concentrations, where the extrachannel entry process is rate limiting, and become more superlinear with higher concentrations.

Under superlinear conditions, replacement of Trp with nonpolar Phe (Bamberg et al., 1976; Heitz et al., 1982, 1986; Becker et al., 1991) or naphthylalanine (Daumas et al., 1989; Fonseca et al., 1992) reduces conductance for the alkali metal cations. This result is expected because the polar Trp side chains, which are situated out of contact with the permeation pathway ~7 Å lateral to the inner wall of the channel, are oriented with their indole dipole moments approximately parallel to the permeation pathway. This dipole orientation is the opposite of the orientation of the effective dipole from the lipid headgroups and associated waters, and thus counters their interfacial dipole potential (IDP). For cations, the IDP adds to the desolvation barrier to inhibit translocation (if anions were permeant, the IDP would subtract from the desolvation barrier because of its dipolar character). Trp side-chain dipole potential appears to reduce this overall barrier for cations (and presumably increase it for anions) (Sancho and Martínez, 1991; Hu and Cross, 1995; Woolf and Roux, 1997; Dorigo et al., 1999) by reducing the potential barrier at the bilayer center due to the negative end of the indole dipole, with perhaps a slight barrier outside the channel entry due to the positive end of the indole dipole.

Increasing the Trp dipole potential by fluorination of the side chain has been shown to increase alkali metal conductance in lecithin bilayers (Andersen et al., 1998; Busath et al., 1998). The same modification decreases alkali metal conductance in monoolein bilayers at moderate ion concentrations, a finding that has been speculated to reflect the dominance of the entry step in these bilayers due to their low IDP (Busath et al., 1998). Solid-state NMR studies demonstrate that in lecithin multilayers Trp side-chain orientations are only modestly affected by fluorination (Cotten et al., 1999), so the conductance changes are probably due to changes in the magnitude or angle of the Trp side-chain dipole moment rather than side-chain orientation. The purpose of this paper is to consider the effect of these noncontact dipole potentials from the polar side chains and the IDP on proton conductance. Our motive is to follow up on the observation made previously (Busath et al., 1998) that proton conductance is reduced by Trp[13] fluorination in both monoolein and lecithin bilayers. That finding raised the questions of whether diffusion up to the channel entry was rate limiting and whether other side-chain polarity changes would give the same effect. The findings reported here answer these questions and raise new questions about the mechanism of proton conductance in the superlinear regime.

Ion-free gramicidin channels contain eight or nine water molecules in a single file (Rosenberg and Finkelstein, 1978; Levitt et al., 1978; Levitt, 1984; Tripathy and Hladky, 1998), which are free to interact and rotate. The waters thus form an ideal "proton wire" (Nagle and Morowitz, 1978), with fully aligned dipole moments as the lowest energy conformation (Partenskii et al., 1991). Channel permeability to protons is 40- to 60-fold higher than permeability to Na^+ (Myers and Haydon, 1972), and single-channel proton conductance at infinite dilution is 9.1-fold higher than Na^+ conductance (Hladky and Haydon, 1972). Water flux is not induced by proton-mediated currents, as it is with alkali metal currents (Levitt et al., 1978). Thus proton transport through the gA channel occurs by means of Grotthuss conductance (Myers and Haydon, 1972).

A theoretical analysis of proton transport in a nine-water wire in vacuo emphasizes the difference between the time scales for proton passage ($<$ ps) and the subsequent water reorientation ($>$ ns) (Pomès and Roux, 1998). Positive charge transport first requires that a (hydrated) proton approach a channel containing a water column aligned with water oxygens toward the channel entry. After rapid exchange of hydrogen bonds and covalent bonds, which results in the release of a hydrogen at the channel exit, the water column has become aligned in the opposite direction and must completely reorient before the next proton transport can occur. Reorientation is expected to be rate-limiting and occurs by propagation of a hydrogen-bonding defect through the channel. The transition state occurs when the defect reaches the center of the channel and has an activation energy, due to oppositely directed channel water hemicolumns, of ~8 kcal/mol (Pomès and Roux, 1998). This

barrier computed in vacuum is reduced in the more disordered gA channel, but is still several kcal/mol (R. Pomès and B. Roux, personal communication).

Several experimental studies of proton conductance properties in gramicidin channels have been carried out (Hladky and Haydon, 1972; Eisenman et al., 1978, 1980; Heinemann and Sigworth, 1989; Akeson and Deamer, 1991; Cukierman et al., 1997). The *I-V*s have been found by Eisenman et al. (1980) to be sublinear for glyceryl monoolein (GMO) bilayers in HCl solutions of pH $>$ 2 and to be superlinear for pH $<$ 2, with superlinearity peaking at pH 1 and then declining toward linearity at pH -1. The switchover between 0.01 M and 0.1 M was confirmed by Akeson and Deamer (1991). By comparison to the conductance behaviors of ion carriers (Krasne and Eisenman, 1977), the shift from sub- to superlinear implies a switchover from entry-limited transport to translocation-limited transport (Eisenman et al., 1980).

It should be noted that in the same concentration range (~pH 2) there is a plateau in the conductance-activity curve followed by a secondary rise (Eisenman et al., 1980). The curve was constructed from several data sources, so some caution must be exercised in its interpretation. If real, the secondary rise could be considered to be evidence of enhanced exit in a doubly occupied, single-file pore (Hille and Schwarz, 1978). Schumaker et al. (1999) have recently estimated that the rate of water column reorientation predicted by molecular dynamics is consistent with the initial rise and plateau in the measured proton conductance-activity curve. The model did not predict a secondary rise, suggesting the involvement of additional processes such as second-proton entry. Although the results reported here are interpreted mainly in terms of water reorientation limitations on proton transport, the plateau phenomenon merits further research and may extend our conclusions.

Here we report proton conductance of homodimeric channels formed from several gA analogs in two lipid bilayers of different IDP, utilizing $[H^+]$ above and below the plateau region identified by Eisenman et al. (1980), focusing especially on the superlinear regime. The analogs include the Trp-to-Phe variants gramicidin B (gB = W11F gA), gramicidin M (gM = W9, 11, 13, 15F gA), and W9,11F gA. In addition, three indole-C5 fluorinated Trp analogs (fgAs) were used, namely, fluorinated Trp[15] gA (fW15 gA), Trp[13] gA (fW13 gA), and Trp[11] gA (fW11 gA). We will show that the anomalous effect of interfacial dipoles on H^+ conductance is a general phenomenon, confirming a preliminary report on proton conductance in gB (Sandblom et al., 1990). All manipulations of the IDP examined so far, whether they are introduced by changing the lipid headgroup or the peptide side chains located in the interfacial region, have opposite effects on alkali metal cation and proton conduction in the superlinear regime. Although there are differences between the mechanisms of alkali metal cation transport and Grotthuss transport, the observation of opposing interfacial dipole effects argues against the possibility that Grotthuss conductance is limited

by the movement of positive charge across the channel in this regime, because monovalent cation movement through the channel should be modulated in the same direction by interfacial dipoles independent of the ion species. We will discuss alternative explanations involving anion-dipole and dipole-dipole interactions and briefly suggest a possible explanation for the secondary rise in the proton conductance-activity curve involving ion-stimulated water reorientation.

MATERIALS AND METHODS

HCl (Fisher, Fair Lawn, NJ) was diluted from concentrate, using distilled water purified to >18 MΩ-cm with a Barnstead NANOpure II system (VWR Scientific, San Francisco, CA). pH measurements were performed with a Corning pH/ion analyzer (model 350; Fisher Scientific, Pittsburgh, PA). GMO (NuChek Prep, Elysian, MN), diphytanoyl phosphatidylcholine (DPhPC), (Avanti Polar Lipids, Birmingham, AL), and n-hexadecane and n-decane (Aldrich, Milwaukee, WI) were used without additional purification. All lipid solutions were used for 1–4 weeks and then discarded.

gA was purchased from ICN Biomedicals (Aurora, OH) and used without further purification. fgAs, W9,11F gA, and gM (all with isotopic labels for other purposes) were synthesized by solid-phase synthesis as described previously (Busath et al., 1998; Fields et al., 1988, 1989). gB was purified from gramicidin D (ICN Biomedicals) by isocratic high-performance liquid chromatography. Peptide solutions were prepared in methanol (Fisher Scientific, Fair Lawn, NJ) and diluted in 10-fold increments to 10^{-5} mg/ml ($\sim$5 nM). Channel frequencies of $\sim$10–30 min^{-1} were obtained by injecting the 2–3-ml bath with 40–80 pg gA, $\sim$400 pg gB, 40–60 pg 5fW11 gA, 40–80 pg 5fW13 gA, $\sim$4000 pg 5fW15 gA, 200 pg W9,11F gA, or 2000–4000 pg gM.

Lipid bilayers were formed and channel properties measured as reported previously (Busath et al., 1998). Briefly, bilayers were painted on an aperture from dispersions of GMO in hexadecane (50 mg/ml) or DPhPC in decane (20 mg/ml). Membrane potentials were applied with Ag-AgCl electrodes, and currents were measured with a Warner BC-525C Bilayer Clamp (Warner Instruments, Hamden, CT) or a List EPC7 patch-clamp amplifier (List Medical, Darmstadt, Germany). The bilayer current was low-pass filtered with a cutoff frequency of 100 Hz and collected continuously for 10–30 min, using IGOR Pro (Version 3.01; Wave Metrics, Lake Oswego, OR). Current transitions were analyzed with the computer programs TAC and TACfit (Version 2.5; Skalar Instruments, Seattle, WA).

The single-channel current histograms contained channels with abnormally low and high conductances, although most fall within an approximately bell-shaped curve. Histograms were fitted with two Gaussian curves, one for the predominant species and one small broad peak for the variant channels. The means of the predominant peaks from three or more experiments were normalized to a 23°C room temperature, using $Q_{10} = 1.38$ (Hladky and Haydon, 1972), and averaged, using the standard deviations of the fitted normal curves as weighting factors. Temperature corrections rarely exceeded 2°C. If the standard deviation among experiments was unusually high (>0.15 pA), the experiments were repeated. Interexperimental standard deviations were typically 2–5% of the conductance after temperature correction, presumably because of deviations from the nominal bath concentration and temperature.

RESULTS

Single-channel currents appear to be stable in HCl, as is illustrated by the single-channel current trace and current transition histogram for gA shown in Fig. 1 B, which are similar to those previously published (Haydon and Hladky, 1972; Heinemann and Sigworth, 1989; Akeson and Deamer, 1991; Cukierman et al., 1997). Fig. 1, A and C, shows that the histogram and channel proton currents are similar but
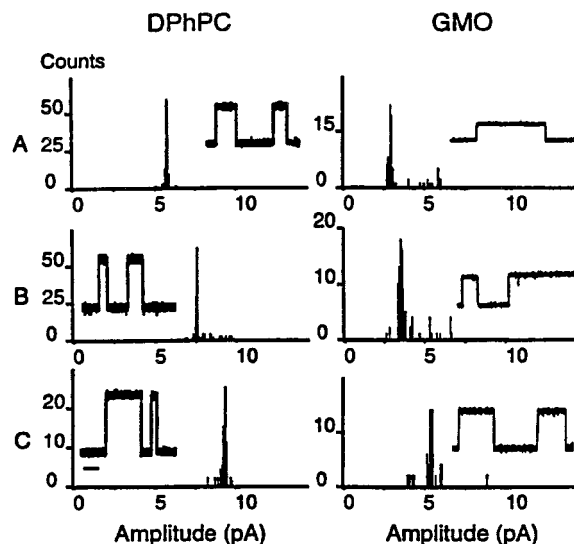

FIGURE 1 Single channel currents (standard channels only) and histograms for fW13 gA (A), gA (B), and gB (C) in DPhPC (*left column*) and in GMO (*right column*) with 0.1 N HCl at 50 mV. The time scale bar in the lower left-hand corner of C represents 1 s for the current traces. The single-channel conductances in the current traces are represented by the accompanying histogram peaks. 23 $\pm$ 1°C.

reduced and increased, respectively, for fW13 gA and gB, contrary to expectations from alkali metal cation conductances. Similar behavior was observed for fW11 gA and fW15 gA in both lipids, for W9,11F gA in DPhPC bilayers, and for gM in GMO bilayers. W9,11F gA also formed discrete, stable channels in GMO bilayers, but with very heterogeneous conductance distributions. gM formed single channels of approximately normal lifetimes in DPhPC bilayers, but with excessively variable conductances. These two combinations are therefore not considered further in this report.

Fig. 2 displays the I-Vs for five different peptides in GMO with symmetrical 0.1 N HCl baths. In multiple instances where the I-Vs were measured up to 200 mV for this and subsequent I-Vs (data not shown), there was no deviation from the patterns shown here. There is a progression of conductances, with gB > gA > fW11 gA $\approx$ fW15 gA > fW13 gA. Fig. 3 A shows the I-Vs for gA and fW13 gA in GMO with a [HCl] of 0.18 N (pH 0.75). The gA conductances are increased compared to those in 0.1 N HCl because of the higher bath [H^{+}]. The two peptides follow the same sequence at the higher concentration as in Fig. 2, with gA having a higher conductance than fW13 gA. Fig. 3 B contains the I-Vs for gA and fW13 gA in GMO at a concentration of 0.018 N (pH 1.75). Note the decreased conductance of both I-Vs compared to their respective traces in Fig. 2. Again, the gA conductance is higher than that of fW13 gA.

Fig. 4 shows I-Vs for the same peptides as in Fig. 2 with 0.1 N HCl in DPhPC bilayers. In this case, the fW13 gA and fW15 gA I-Vs are nearly indistinguishable from each other (rather than fW11 gA and fW15 gA as in GMO bilayers),
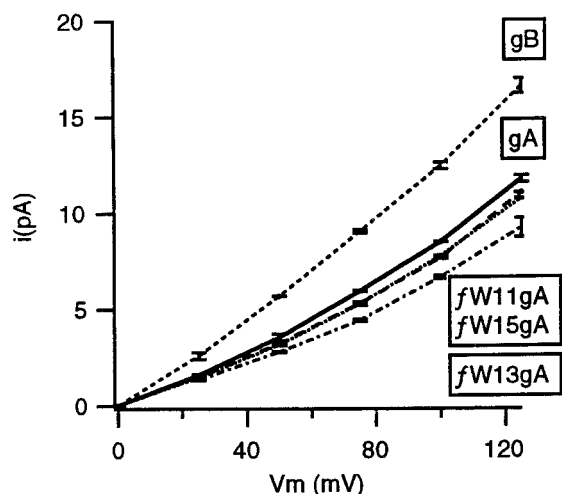
FIGURE 2 Mean single standard channel *I-V* for gB, gA, *f*W11 gA, *f*W13 gA, and *f*W15 gA in GMO/hexadecane bilayers. 0.1 N HCl, 23 ± 1°C. *f*W11 gA and *f*W15 gA had almost identical conductances.

FIGURE 4 Mean single standard channel *I-V* for gB, gA, and *f*W11 gA, *f*W13 gA, and *f*W15 gA in DPhPC/decane bilayers. 0.1 N HCl, 23 ± 1°C.

but otherwise the same progression of conductances occurs as in GMO bilayers. Fig. 5, *A* and *B*, shows gA and *f*W13 gA *I-V*s with 0.18 N and 0.018 N HCl, respectively, as in Fig. 3, but in DPhPC bilayers. Again gA has a higher conductance than *f*W13 gA at both [HCl] levels, which is the opposite of the result found for alkali metal cations (Busath et al., 1998). For each peptide the specific conductivity (conductance/activity) in DPhPC is higher than that in GMO, which is also the opposite of the lipid effect for alkali metal cations (Busath et al., 1998). Furthermore, the lower [HCl] (Fig. 5 *B*) yields a sublinear gA *I-V* in DPhPC bilayers, but not in GMO bilayers. This contrasts with the *I-V* shape sequences observed for alkali metal cations for these two lipids (Busath et al., 1998), where *I-V*s at low ion concentrations are sublinear in GMO but not in DPhPC.

Table 1 shows the single-channel conductances at 50 mV in 0.1 N HCl and at 100 mV in 1 M KCl for the peptides described above as well as for gM in GMO and W9,11 gA in DPhPC (see above). The H^+ conductances in DPhPC are uniformly higher than those in GMO, contrary to the K^+ conductances. Likewise, H^+ conductances increase as side-chain polarity decreases, again contrary to the progression seen in KCl solutions. The disparity between H^+ and K^+
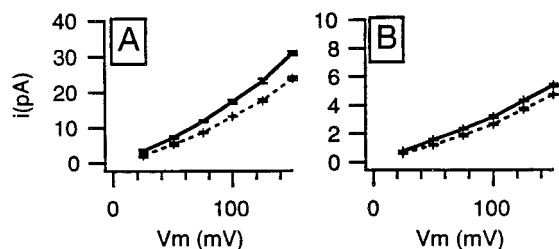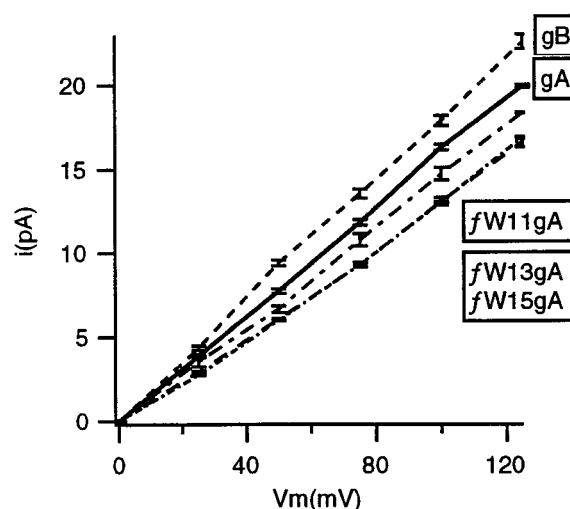
conductances becomes most obvious in the bottom two rows of Table 1, where only two or no Trps are present.

DISCUSSION

The H^+ conductance of gA analogs follows the sequence gM > gB > gA > *f*gA in GMO and gB > W9,11F gA > gA > *f*gA in DPhPC, which, except for the first pair in DPhPC, is the opposite of those sequences observed for K^+ conductances and follows the side-chain polarity sequence. For any given peptide, the H^+ conductance was higher in DPhPC than in GMO, which is also contrary to the effect on K^+ and Na^+ conductance (Busath et al., 1998). These observations held over the concentration range explored here (0.018, 0.1, 0.18 N HCl). The rate-limiting factor in H^+ transport is apparently modulated in the direction opposite that governing alkali metal cations by changes in the analog side chains or lipid headgroups, suggesting a different mechanism for H^+ transport through the channel. For increasing side-chain dipole moment, the H^+ transport rate decreases, whereas the K^+ transport rate increases.

Previous related findings

The concept that the rate-limiting process switches from an extrachannel to an intrachannel process between HCl con-

FIGURE 3 Mean single standard channel *I-V* for gA (*solid lines between points*) and *f*W13 gA (*dashed lines*) in (*A*) 0.18 N HCl and (*B*) 0.018 N HCl. GMO/hexadecane bilayers, 23 ± 1°C.
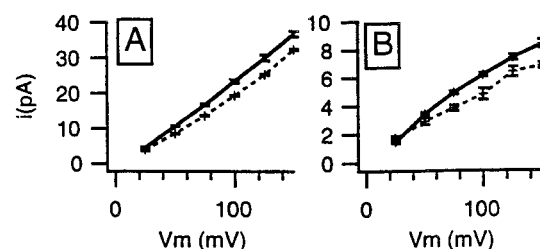

FIGURE 5 Mean single standard channel *I-V* for gA (*solid lines*) and *f*W13 gA (*dashed lines*) in (*A*) 0.18 N HCl and (*B*) 0.018 N HCl. DPhPC/decane bilayers, 23 ± 1°C.

TABLE 1 Single-channel currents (pA)*

	GMO/hexadecane		DPhPC/decane	
	H$^+$	K$^+$	H$^+$	K$^+$
fW15 gA	3.21 ± 0.02	4.73 ± 0.03	5.97 ± 0.04	2.56 ± 0.07
fW13 gA	2.77 ± 0.02	4.42 ± 0.06	6.11 ± 0.07	2.50 ± 0.04
fW11 gA	3.16 ± 0.06	4.82 ± 0.03	6.65 ± 0.21	2.65 ± 0.11
gA	3.81 ± 0.08	4.49 ± 0.08	7.74 ± 0.12	2.11 ± 0.03
gB	5.86 ± 0.17	3.5[#]	9.41 ± 0.18	1.42 ± 0.03
W9, 11F, gA	NS[§]	ND	8.26 ± 0.68	0.58 ± 0.03
gM	6.99 ± 0.06	0.6[∥]	NS	ND

*Mean ± S.E.M. in pA, 0.1 N HCl, 50 mV, 23 C (H$^+$) or 1.0 M KCl, 100 mV, 23 C (K$^+$).

[#]From Bamberg et al. (1976).

[§]NS: Channels not stable or very heterogeneous in conductance; ND: not done.

[∥]From Seoh and Busath (1995).

centrations of 0.01 N and 0.1 N was deduced from *I-V* shapes by Eisenman et al. (1980) and buttressed with measurements of deuteron conductance in 90% D$_2$O by Akeson and Deamer (1991). The conductance in D$_2$O is reduced by a factor of 1.34 ± 0.11 in 0.1 N HCl, which is somewhat below (although not statistically significant) the reduction factor measured in bulk water (1.4) and is reduced by a factor of only 1.20 ± 0.01 in 1.0 N HCl. This was interpreted to imply that D$_2$O reorientation is not as limiting as H$_2$O reorientation in the channel and that the intrachannel process is increasingly rate limiting at the higher concentrations. The rectification and isotope effects are small, so this interpretation must be accepted with some caution. Furthermore, membrane electrostriction or small potential drops in the bulk solution (Laüger, 1976, Peskoff and Bers, 1988) could contribute to the voltage dependence of the current. However, membrane potential primarily alters ion flow within the channel.

The effect of lipid headgroups is evident in the recent study of Cukierman et al. (1997). Before we consider possible surface charge effects, we note that the results are the opposite of those reported here, in that the proton conductance in bilayers composed of 1-palmitoyl-2-oleoyl-phosphatidylethanolamine (80%) and 1-palmitoyl-2-oleoyl-phosphatidylcholine (20%) in decane (PE/PC) was lower than in GMO/decane (their figure 9, right). After correction for surface potential effects due to expected protonation of the phospholipid headgroups, assuming a pK$_a$ of 1.0 for phosphates (an upper bound suggested by Marsh, 1990), the gA-specific conductance is higher in PE/PC, which is similar to our observations of increased proton conductance in DPhPC bilayers, even without any correction for membrane protonation. It should be noted, however, that Cukierman et al. found the conductance in GMO to rise above that in PE/PC at concentrations above 2.0 N HCl, which is not entirely explained by the current models. It is clear that additional experiments are needed, with better evaluation of headgroup protonation (for instance, using direct measures of protonation to account for shifts in phosphate pK$_A$) and considering the relative roles of protonation on reduction of

cation concentration in the bulk versus lateral proton diffusion in the plane of the bilayer.

Implications of current results

A great deal has been published on the quantum and classical mechanics of Grotthuss H$^+$ transport (e.g., Bjerrum, 1952; Knapp et al., 1980; Nagle and Tristram-Nagle, 1983; Scheiner, 1985; Nagle, 1987; Deamer, 1987; Pnevmatikos, 1988; Bala et al., 1994; Prokop and Skála, 1994; Mavri and Berendsen, 1995; Sagnella and Voth, 1996; Sagnella et al., 1996; Pomès and Roux, 1996, 1998; Schmidt and Brickmann, 1997; Mei et al., 1998; Marx et al., 1999; Dècornez et al., 1999). It is generally agreed that Grotthuss conductance is a two-step process consisting of a fast rearrangement of hydrogen bonds and covalent bonds, which yields the formal positive charge movement, followed by a slower reorientation of waters required to realign the hydrogen bond network for the next proton passage. It is conceivable that in the gramicidin channel the movement of negative charge (such as a hydroxide, an electron, or concerted water oxygens pivoting about their hydrogen-bond stabilized protons) is rate limiting for proton conductance, and thus proton transport is affected by axial dipole potentials in the direction opposite that of cation transport, as suggested by hydrophobic cation and anion transport studies in planar bilayers (Hladky and Haydon, 1973; Pickar and Benz, 1978; Cseh and Benz, 1998).

Prior theoretical studies of proton transport in gramicidin channels have focused on the hydration of the proton (Sagnella and Voth, 1996; Sagnella et al., 1996; Pomès and Roux, 1996). Of greater importance here, however, is the water wire study by Pomès and Roux (1998) that focused on the slow water reorientation after H$^+$ transfer. After the fast step, in which the H$^+$ is transferred from entry to exit by way of an aligned water chain (Fig. 6 *A*), the water chain is left with all dipoles oriented in the opposite direction, i.e., with all dipoles pointing toward the entry (Fig. 6 *B*). We will refer to this posttransport configuration as an "inactive state" of the water column because the next left-to-right H$^+$ transport cannot take place until the water column reverses dipole orientation so that all of the dipoles face the exit, i.e., the oxygens face the entry and are ready to receive another incoming proton. Molecular dynamics computations using a collective reaction coordinate for umbrella sampling (Pomès and Roux, 1998) indicate that the reorientation usually begins with the rotation of a water near one end, forming a hydrogen-bonding defect. This defect then propagates to the center of the channel, the transition state, at which point the water wire consists of two half-columns with oppositely pointing dipoles. The transition barrier to water reorientation is expected to be rate limiting for proton transport (Pomès and Roux, 1998; Schumaker et al., 1999).

We reason that if the defect starts at the entry, then the dipoles on the left-hand side of the column in Fig. 6 *B* reorient first, until the transition state illustrated in Fig. 6 *C*

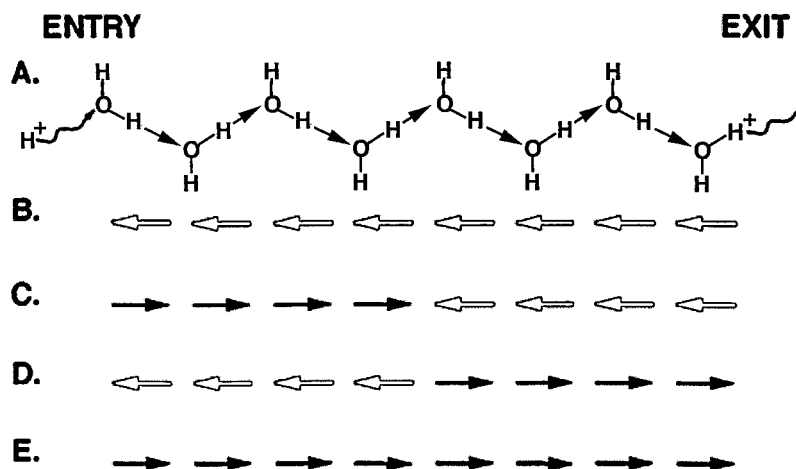**ENTRY**   **EXIT**

FIGURE 6   Diagram illustrating water orientation changes associated with proton transport in the conventional Grotthuss paradigm. (*A*) Water column modification due to H^+ transport from left to right. The proton on the far left diffuses into the entry of a channel containing a properly oriented water column, initiating transport. Each water passes a proton rightward along the hydrogen bond (*straight arrow*). The H^+ from the final water diffuses away from the exit. The water dipoles in the column are then oriented in the opposite direction. (*B*) Water dipole alignment after H^+ transport, inappropriate for another left-to-right H^+ transport. (*C*) Transition state dipole alignment after defect origination at the channel entry (*left*). (*D*) Transition state dipole alignment after defect origination at the channel exit (*right*). (*E*) Water dipole alignment after water column reorientation step. The column is now prepared to transport the next proton. Dipoles are rendered as filled or open arrows for visual contrast only.

is reached. If the defect starts at the exit, then the dipoles on the right-hand side in Fig. 6 *B* reorient first, resulting in the transition state illustrated in Fig. 6 *D*. In both cases, the reaction then proceeds to completion by defect propagation through the remainder of the column (Fig. 6 *E*). In this process, the dipole moment for a nine-water column varies from -7.75 eÅ (Fig. 6 *B*) to 0 eÅ (Fig. 6, *C* or *D*), to $+7.75$ eÅ (Fig. 6 *E*) (Pomès and Roux, 1998). The result of Pomès and Roux suggests a new dipole/water-dipole interaction hypothesis for the modulation of proton transport in gramicidin channels, which we propose below after first briefly introducing an alternative dipole/negative-charge interaction hypothesis.

Dipole/negative-charge interaction hypothesis

As mentioned above, from the perspective of studies done with hydrophobic anions and cations, for which the electrophoretic mobility changes in opposite directions in response to changes in IDP (Hladky and Haydon, 1973; Pickar and Benz, 1978; Cseh and Benz, 1998), it is natural to wonder if negative charge movement is rate limiting for H^+ transport in gramicidin channels. OH^- or an aqueous electron derived from water splitting at the channel exit, perhaps under the influence of a high membrane field and high $[Cl^-]$ in the exit bath, could translate to the channel entry and there annihilate a H^+. Alternatively, water reorientation may be associated with charge movement (Nagle and Morowitz, 1978). Perhaps water OH could pivot about H hydrogen-bonded to the channel wall, yielding negative charge movement. In each case, the IDP would then facilitate negative charge transfer across the membrane, as it does with hydrophobic anion transport in planar bilayers. The water splitting hypothesis, however, seems unlikely,

given the basicity of OH^- relative to Cl^-. Furthermore, Busath et al. (1998) reported that in asymmetrical 1 M guanidinium chloride//1 M KCl solutions, gA channels are completely impermeable when the positive potential is applied to the guanidinium chloride bath. One would think that Cl^--induced water splitting could have occurred under these conditions and rendered the channel conductive because the exit bath contained 1 M KCl. Careful consideration of water reorientation suggests that associated moving charges would be predominantly protonic, whether or not one proton is hydrogen-bonded to the channel wall.

Dipole/water-dipole interaction hypothesis

We therefore focus instead on a completely different paradigm for H^+ current modulation by interfacial dipoles, which seems to have a compelling richness and simplicity. In this mechanism, interfacial dipoles regulate the water column reorientation, which is propagated by Bjerrum defects in the hydrogen-bonding pattern. The rate of water reorientation is modulated by interactions between interfacial dipoles and the intrachannel water dipoles. This is illustrated in Fig. 7, which shows the interfacial dipoles due to the lipid headgroups at the bilayer surfaces and the applied potential as positive on the left. The gA channels, with dipolar side chains pointing toward the aqueous phase, as determined by NMR (Arsenyev et al., 1990; Koeppe et al., 1994; Hu et al., 1995), have water dipoles in the inactive configuration (after a proton transport, *top*), the transition configuration (after partial water reorientation starting at the exit, *middle*), and the fully reoriented active configuration (*bottom*).

To begin, we propose that it is likely that water reorientation is initiated at the exit for two reasons. First, for the

FIGURE 7 Diagram illustrating dipole/water-dipole interaction hypothesis for anomalous interfacial dipole effects on proton transport. The dipoles associated with lipid headgroups are shown along the membrane surface as the *largest arrows*, with the monolayer interfacial potential of ~300 mV labeled at the top. A membrane potential applied with the positive terminal of a battery on the left, ground on the right, would cause positive charge flow from left to right. The side-chain dipoles (Trp[9], Trp[11], Trp[13], and Trp[15] in gA) are shown as *small circled arrows* in their known orientations, opposite the lipid headgroup dipoles. *Top*: After proton transport (depicted by *wavy arrows*), the water column is in the "inactive state," i.e., with all water dipoles (shown as *arrows* in the channel) facing the entry. The water near the exit is most destabilized by the parallel dipoles of the lipid headgroups (as depicted by the *curved arrows*) and is therefore likely to be the origin of the hydrogen-bonding defect that initiates reorientation of the water column. Defect formation should be stimulated by membrane potential (positive at the channel entry, negative at the exit), chloride ion accumulation near the exit due to interfacial polarization produced by the membrane potential, and increased [Cl$^-$] associated with increases in bath [HCl]. It would be inhibited by antiparallel side-chain dipoles, causing the anomaly that is the focus of this paper. *Middle*: The "transition state" for an exit-initiated defect has both water hemicolumns antiparallel to, and thus stabilized, by the lipid headgroup dipoles in the nearest monolayer surface. The opposite is true for an entry-initiated defect transition state (Fig. 6 *C*). Side-chain dipoles destabilize the exit-initiated transition state by unfavorable interactions between each monomer and its luminal hemicolumn. They would therefore inhibit water reorientation and H$^+$ conductance, as reported here. *Bottom*: Upon completion of reorientation the water chain is in the "active state," i.e., it is prepared for transport of another H$^+$.
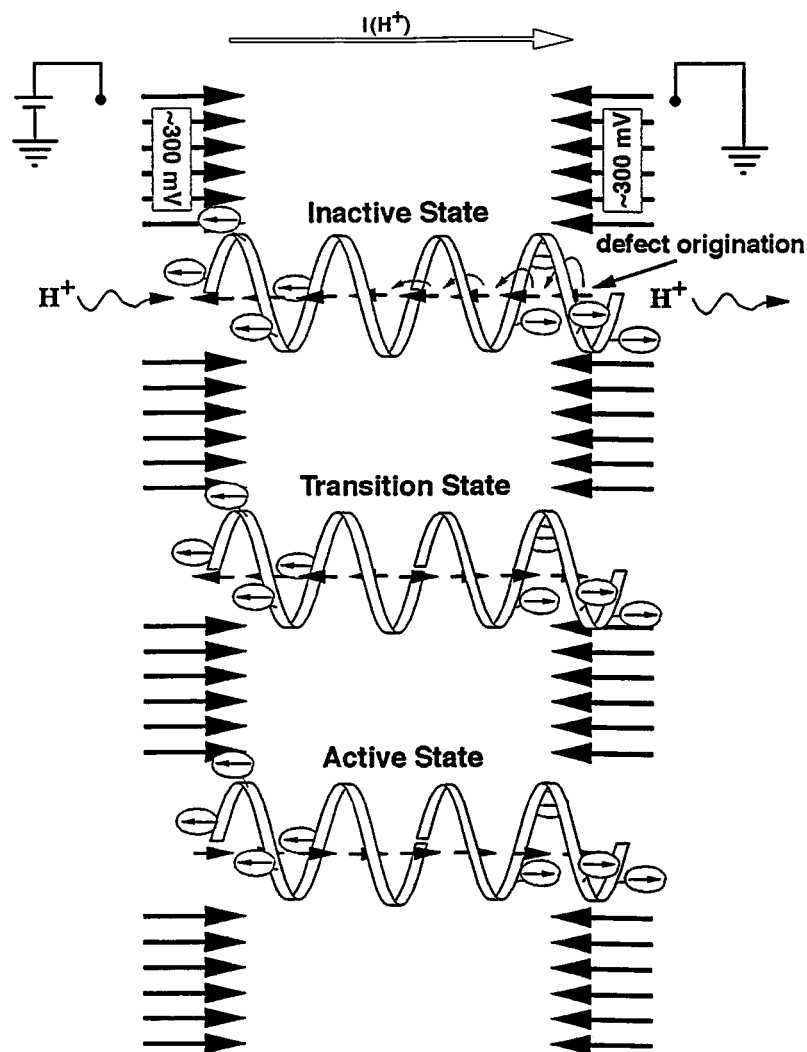
inactive configuration the dipole potential from the lipid headgroups on the exit-side monolayer should destabilize the waters near the exit, whereas the entry-side monolayer potential would stabilize the channel waters near the entry, as illustrated by the curved arrows on the inactive state waters (Fig. 7, *top*). The destabilization is expected because the effective headgroup dipole is parallel to the water dipole, which is energetically less favorable than if the two dipoles are antiparallel. We assume that the water dipole is in equilibrium between the two states (despite the energy barrier presented by the unfavorable perpendicular orientation) as a result of thermal vibrations. The magnitude of the IDP measured with monolayers, an approximation to that found in each interface in lipid bilayers, is 274 for GMO and 390 mV for dioleoylphosphatidylcholine, which approximates that of DPhPC (Pickar and Benz, 1978). The IDP would be transmitted with moderate attenuation (~50%, Jordan, 1984) to the center of the channel. Second, the transition state, where two antiparallel water hemicolumns are joined by a hydrogen-bond defect at the center of the bilayer, would be stabilized by interactions with the monolayer potentials on each side of the channel if the hemicol-

umns point away from each other (exit defect origin, Fig. 6 *D*), whereas it would be destabilized if the hemicolumns point toward each other (entry defect origin, Fig. 6 *C*). Therefore, propagation of an exit-origin defect across the channel would be more favorable energetically than propagation of an entry-origin defect based on the opposing monolayer dipole potentials.

Next we claim that the origin of the defect determines the expected effect of the interfacial dipoles on the rate of water reorientation. With an exit-origin reorientation, increased lipid IDP and decreased peptide side-chain dipoles increase H$^+$ conductance because they would destabilize the waters at the exit, speeding defect origination. Furthermore, they would stabilize the transition state, in accord with the results reported here. Both effects would increase the rate of water reorientation. On the other hand, if the hydrogen bond defect started at the entry, increased lipid IDP and decreased peptide side-chain dipoles would reduce the rate of water reorientation and thus H$^+$ conductance, contrary to the results reported here.

Recognizing that the exit-initiated water reorientation model qualitatively predicts the dipole effects we report, we

must next address two more fundamental questions: 1) Why would reorientation of the water column be voltage dependent, producing increasing H^+ flux at increased voltages and superlinear I-Vs at high [HCl]? and 2) Why does H^+ flux increase with bath [HCl] when water reorientation is rate limiting? We suggest the following straightforward explanations. The applied potential (Fig. 7) destabilizes the inactive state, so the water reorientation rate increases with V_m. The energy of the transition state (in which μ, the net dipole moment of the water column, is 0 e·Å), relative to the inactive state ($\mu = 7.75$ e·Å) (Pomès and Roux, 1998), would vary (at applied potentials above ~50 mV, where back flux is expected to be negligible) according to

$$\Delta G = eV_m \Delta \mu / d \qquad (1)$$

Here e is the elementary charge in coulombs, V_m is the applied potential in volts, and d is the length over which the potential falls, in Å. For the 25-Å-long channel, assuming that the H^+ transport is limited by the reorientation rate, which decreases exponentially with $\Delta G/RT$, the rate is expected to increase e-fold for every 82.3-mV applied potential (or 1.36-fold for every 25 mV) at 23°C, thus yielding a superlinear I-V. This is close to the voltage dependence of the current observed here. For instance, under eight different experimental conditions using different peptides (gA or fW13gA), lipids (GMO or DPhPC), or [HCl] (0.1 N, 0.18 N or 1.0 N), the current at 125 mV exceeded that at 100 mV by an average factor of 1.32 ± 0.04, demonstrating that the voltage dependence was not an artifact of the transport kinetics in one peptide, lipid, or ionic bath.

However, the theory that water reorientation is rate-limiting and exit-initiated as an explanation for the current results raises two interesting issues. First, starting with concentrations of ~0.01 N, there is a secondary rise in the current/concentration plot that has traditionally been ascribed to increasing double occupancy (Eisenman et al., 1980). The onset of superlinearity in the I-V in this concentration range may be a double-occupancy effect: inter-ion repulsion in the doubly occupied channel might be enhanced by membrane potential. Kinetic modeling of the water-reorientation limited proton flux through gA based on single occupancy successfully predicted the initial rise in the current/concentration curve. However, the model predicts that current would reach a plateau above 0.01 N, limited by the gA water reorientation rate predicted from umbrella sampling computations (Schumaker et al., 1999). Similarly, our model requires some mechanism by which proton conductance continues to rise with bath [HCl] up to 4 N. Traditionally, the increasing $[H^+]$ in the entry bath is the expected cause of the rise, but this cannot easily be rationalized with the current theory.

Both of these concerns might conceivably be answered by considering the effect of Cl^- in the exit bath. As the bath [HCl] is increased symmetrically, the exit Cl^- may play an increasing role in facilitating conductance. For instance, Cl^- near the channel exit would repel the dipole of the last

water in the channel and facilitate its reorientation. The facilitation per se would be membrane potential-independent (i.e., extrachannel) but would affect the intrachannel process, water reorientation, and so might be expected to affect the I-V shape. Thus the findings presented here have stimulated novel conceptualizations of proton transport in gA channels and should stimulate new experimental approaches to test them.

SUMMARY

Proton conductance is affected negatively by increased interfacial dipoles in channels formed by gA and related analogs. These effects are well explained by a consideration of the interfacial dipoles on the intrachannel process mediating proton conductance. Water reorientation is thought to be rate limiting for Grotthuss conductance in water wires. Modulation of the intrachannel water reorientation rate, defined here as the dipole/water-dipole interaction model, provides a successful qualitative explanation of the dipole effects. Similar proton conduction effects are likely to play a role in other proteins, where H^+ transport is thought to occur by water wires, such as in the vestibule portions of bacteriorhodopsin and the aqueous channels in the F_0 subunit of F_0F_1-ATPase.

REFERENCES

Akeson, M., and D. W. Deamer. 1991. Proton conductance by the gram-icidin water wire. Model for proton conductance in the F_1F_0 ATPases? *Biophys. J.* 60:101–109.

Andersen, O. S. 1983. Ion movement through gramicidin A channels. Single-channel measurements at very high potentials. *Biophys. J.* 41:119–133.

Andersen, O. S., D. V. Greathouse, L. L. Providence, M. D. Becker, and R. E. Koeppe, II. 1998. Importance of tryptophan dipoles for protein function: 5-fluorination of tryptophans in gramicidin A channels. *J. Am. Chem. Soc.* 120:5142–5146.

Arsenyev, A. S., A. L. Lomize, I. L. Barsukov, and V. F. Bystrov. 1990. Gramicidin A transmembrane channel. Three-dimensional structural rearrangement based on NMR spectroscopy and energy refinement. *Biol. Membr.* 3:1723–1778.

Bala, P., B. Lesyng, and J. A. McCammon. 1994. Applications of quantum-classical and quantum-stochastic molecular dynamics for proton transfer processes. *Chem. Phys.* 180:271–285.

Bamberg, E., K. Noda, E. Gross, and P. Läuger. 1976. Single-channel parameters of gramicidin A, B, and C. *Biochim. Biophys. Acta.* 419:223–228.

Becker, M. D., D. V. Greathouse, R. E. Koeppe, II, and O. S. Andersen. 1991. Amino acid sequence modulation of gramicidin channel function: effects of tryptophan-to-phenylalanine substitutions on the single-channel conductance and duration. *Biochemistry.* 30:8830–8839.

Bjerrum, N. 1952. Structure and properties of ice. *Science.* 115:385–390.

Boyer, P. 1997. The ATP synthase—a splendid molecular machine. *Annu. Rev. Biochem.* 66:717–749.

Busath, D. D., C. D. Thulin, R. W. Hendershot, L. R. Phillips, P. Maughn, C. D. Cole, N. C. Bingham, S. Morrison, L. C. Baird, R. J. Hendershot,

M. Cotten, and T. A. Cross. 1998. Non-contact dipole effects on channel permeation. I. Experiments with (5F-indole)Trp-13 gramicidin A channels. *Biophys. J.* 75:2830–2844.

Cotten, M., C. Tian, D. D. Busath, R. B. Shirts, and T. A. Cross. 1999. Modulating dipoles for structure–function correlations in the gramicidin A channnel. *Biochemistry.* 38:9185–9197.

Cseh, R., and R. Benz. 1998. The adsorption of phloretin to lipid monolayers and bilayers cannot be explained by Langmuir adsorption isotherms alone. *Biophys. J.* 74:1399–1408.

Cukierman, S., E. P. Quigley, and D. S. Crumrine. 1997. Proton conductance in gramicidin A and its dioxolane-linked dimer in different bilayers. *Biophys. J.* 73:2489–2502.

Daumas, P., F. Heitz, L. Ranjalahy-Rasoloarijao, and R. Lazaro. 1989. Gramicidin A analogs: influence of the substitution of the tryptophans by naphthylalanines. *Biochimie.* 71:77–81.

Deamer, D. W. 1987. Proton permeation of lipid bilayers. *J. Bioenerg. Biomembr.* 19:457–479.

Dècornez, H. K. Drukker, and S. Hammes-Schiffer. 1999. Solvation and hydrogen-bonding effects on proton wires. *J. Phys. Chem. A.* 103: 2891–2898.

DeCoursey, T. E., and V. V. Cherny. 1994. Voltage-activated hydrogen ion currents. *J. Membr. Biol.* 141:203–223.

Dorigo, A. E., D. G. Anderson, and D. D. Busath. 1999. Noncontact dipole effects on channel permeation. II. Trp conformations and dipole potentials in gramicidin A. *Biophys. J.* 76:1897–1908.

Eisenman, G., B. Enos, J. Sandblom, and J. Hägglund. 1980. Gramicidin as an example of a single-filing ionic channel. *Ann. N.Y. Acad. Sci.* 339: 8–20.

Eisenman, G., J. Sandblom, and E. Neher. 1978. Interactions in cation permeation through the gramicidin channel. Cs^+, Rb^+, K^+, Na^+, Li^+, Tl^+, H^+, and effects of anion binding. *Biophys. J.* 22:307–340.

Fields, C. G., G. B. Fields, R. L. Noble, and T. A. Cross. 1989. Solid phase peptide synthesis of ^{15}N-gramicidins A, B, and C and high performance liquid chromatographic purification. *Int. J. Pept. Protein Res.* 33: 298–303.

Fields, G. B., C. G. Fields, J. Petefish, H. E. Van Wart, and T. A. Cross. 1988. Solid-phase peptide synthesis and solid-state NMR spectroscopy of $[Ala^3-{}^{15}N][Val^1]$gramicidin A. *Proc. Natl. Acad. Sci. USA.* 85: 1384–1388.

Fonseca, V., P. Daumas, L. Ranjalahy-Rasoloarijao, F. Heitz, R. Lazaro, Y. Trudelle, and O. S. Andersen. 1992. Gramicidin channels that have no tryptophan residues. *Biochemistry.* 31:5340–5350.

Girvin, M. E., V. K. Rastogi, F. Abildgaard, J. L. Markley, and R. H. Fillingame. 1998. Solution structure of the transmembrane H^+-transporting subunit c of the F_1F_0 ATP synthase. *Biochemistry.* 37: 8817–8824.

Haydon, D. A., and S. B. Hladky. 1972. Ion transport across thin lipid membranes: a critical discussion of mechanisms in selected systems. *Q. Rev. Biophys.* 5:187–282.

Heinemann, S. H., and F. J. Sigworth. 1989. Estimation of Na^+ dwell time in the gramicidin A channel. Na^+ ions as blockers of H^+ currents. *Biochim. Biophys. Acta.* 987:8–14.

Heitz, F., C. Gavach, G. Spach, and Y. Trudelle. 1986. Analysis of the ion transfer through the channel of 9,11,13,15-phenylalanylgramicidin A. *Biophys. Chem.* 24:143–148.

Heitz, F., G. Spach, and Y. Trudelle. 1982. Single channels of 9, 11, 13, and 15-destryptophyl-phenylalanyl-gramicidin A. *Biophys. J.* 40:87–89.

Hille, B., and W. Schwarz. 1978. Potassium channels as multi-ion single-file pores. *J. Gen. Physiol.* 72:409–442.

Hladky, S. B., and D. A. Haydon. 1972. Ion transfer across lipid membranes in the presence of gramicidin A. I. Studies of the unit conductance channel. *Biochim. Biophys. Acta.* 274:294–312.

Hladky, S. B., and D. A. Haydon. 1973. Membrane conductance and surface potential. *Biochim. Biophys. Acta.* 318:464–468.

Hladky, S. B., and D. A. Haydon. 1984. Ion movements in gramicidin channels. *Curr. Top. Membr. Transp.* 21:327–372.

Hu, W., and T. A. Cross. 1995. Tryptophan hydrogen bonding and electrical dipole moments: functional roles in the gramicidin channel and implications for membrane proteins. *Biochemistry.* 34:14147–55.

Hu, W., Lazo, N. D., and T. A. Cross. 1995. Tryptophan dynamics and structural refinement in a lipid bilayer environment: solid state NMR of the gramicidin channel. *Biochemistry.* 34:14138–14146.

Jordan, P. C. 1984. The total electrostatic potential in a gramicidin channel. *J. Membr. Biol.* 78:91–102.

Knapp, E. W., K. Schulten, and Z. Schulten. 1980. Proton condution in linear hydrogen-bonded systems. *Chem. Phys.* 46:215–229.

Koeppe, R. E., J. A. Killian, and D. V. Greathouse. 1994. Orientations of the tryptophan 9 and 11 side chains of the gramicidin channel based on deuterium nuclear magnetic resonance spectroscopy. *Biophys. J.* 66: 14–24.

Krasne, S., and G. Eisenman. 1977. Influence of molecular variations of ionophore and lipid on the selective ion permeability of membranes. I. Tetranactin and the methylation of nonactin-type carriers. *J. Membr. Biol.* 30:1–44.

Lanyi, J. K. 1995. Bacteriorhodopsin as a model for proton pumps. *Nature.* 375:461–463.

Laüger, P. 1976. Diffusion-limited ion flow through pores. *Biochim. Biophys. Acta.* 445:493–509.

Levitt, D. G. 1984. Kinetics of movements in narrow channels. *Curr. Top. Membr. Transp.* 21:181–197.

Levitt, D. G., S. R. Elias, and J. M. Hautman. 1978. Number of water molecules coupled to the transport of sodium, potassium and hydrogen ions via gramicidin, nonactin or valinomycin. *Biochim. Biophys. Acta.* 512:436–451.

Marsh, D. 1990. CRC Handbook of Lipid Bilayers. CRC Press, Boca Raton, FL.

Marx, D., M. E. Tuckerman, J. Hutter, and M. Parrinello. 1999. The nature of the hydrated excess proton in water. *Nature.* 397:601–604.

Mavri, J., and H. J. C. Berendsen. 1995. Calculation of the proton transfer rate using density matrix evolution and molecular dynamics simulations: inclusion of the proton excited states. *J. Phys. Chem.* 99:12711–12717.

Mei, H. S., M. E. Tucklerman, D. E. Sagnell, and M. L. Klein. 1998. Quantum nuclear *ab initio* molecular dynamics study of water wires. *J. Phys. Chem. B.* 102:10446–10458.

Moore, W. J. 1972. Physical Chemistry. Prentice-Hall, Englewood Cliffs, NJ.

Myers, V. B., and D. A. Haydon. 1972. Ion transfer across lipid membranes in the presence of gramicidin A. II. The ion selectivity. *Biochim. Biophys. Acta.* 274:313–322.

Nagle, J. F. 1987. Theory of passive proton conductance in lipid bilayers. *J. Bioenerg. Biomembr.* 19:413–426.

Nagle, J. F., and H. J. Morowitz. 1978. Molecular mechanisms for proton transport in membranes. *Proc. Natl. Acad. Sci. USA.* 75:298–302.

Nagle, J. F., and S. Tristram-Nagle. 1983. Hydrogen bonded chain mechanisms for proton conduction and proton pumping. *J. Membr. Biol.* 74:1–14.

Partenskii, M. B., M. Cai, and P. C. Jordan. 1991. A dipolar chain model for the electrostatics of transmembrane ion channels. *Chem. Phys.* 153: 125–131.

Peskoff, A., and D. M. Bers. 1988. Electrodiffusion of ions approaching the mouth of a conducting membrane channel. *Biophys. J.* 53:863–875.

Pickar, A. D., and R. Benz. 1978. Transport of oppositely charged lipophilic probe ions in lipid bilayer membranes having various structures. *J. Membr. Biol.* 44:353–376.

Pnevmatikos, S. 1988. Soliton dynamics of hydrogen-bonded networks: a mechanism for proton conductivity. *Phys. Rev. Lett.* 60:1534–1537.

Pomès, R., and B. Roux. 1996. Structure and dynamics of a proton wire: A theoretical study of H^+ translocation along the single-file water chain in the gramicidin A channel. *Biophys. J.* 71:19–39.

Pomès, R., and B. Roux. 1998. Free energy profiles for H^+ conduction along hydrogen-bonded chains of water molecules. *Biophys. J.* 75: 33–40.

Prokop, P., and L. Skála. 1994. Theory of proton transport along a hydrogen bond chain in an external field. *Chem. Phys. Lett.* 223:279–282.

Rosenberg, P. A., and A. Finkelstein. 1978. Interaction of ions and water in gramicidin A channels. *J. Gen. Physiol.* 72:327–340.

Sagnella, D. E., K. Laasonen, and M. L. Klein. 1996. Ab initio molecular dynamics study of proton transfer in a polyglycine analog of the ion channel gramicidin A. *Biophys. J.* 71:1172–1178.

Sagnella, D. E., and G. A. Voth. 1996. Structure and dynamics of hydronium in the ion channel gramicidin A. *Biophys. J.* 70:2043–2051.

Sancho, M., and G. Martínez. 1991. Electrostatic modeling of dipole-ion interactions in gramicidin like channels. *Biophys. J.* 60:81–88.

Sandblom, J. P., R. M. Josefsson, and T. Larsson. 1990. Some properties of channels formed by gramicidin A and B, including their hybrid forms, in the presence of protons. *In* 10th International Biophysics Congress, Abstracts, International Union of Pure and Applied Biophysics. 391.

Scheiner, S. 1985. Theoretical studies of proton transfers. *Acc. Chem. Res.* 18:174–180.

Schmidt, R. G., and J. Brickmann. 1997. Molecular dynamics simulation of the proton transport in water. *Ber. Bunsenges. Phys. Chem.* 101:1816–1827.

Schumaker, M. F., R. Pomès, and B. Roux. 1999. A combined molecular dynamics and diffusion model of single-proton conduction through gramicidin. *Biophys. J.* 76:A442.

Seoh, S., and D. Busath. 1995. Gramicidin tryptophans mediate formamidinium-induced channel stabilization. *Biophys. J.* 68:2271–2279.

Tripathy, S., and S. B. Hladky. 1998. Streaming potentials in gramicidin channels measured with ion-selective electrodes. *Biophys. J.* 74:2912–2917.

Woolf, T. B., and B. Roux. 1997. The binding site of the gramicidin A channel: comparison of molecular dynamics with solid-state NMR data. *Biophys. J.* 5:1930–1945.